

earth also contains an appreciable amount of water, either dissolved or chemically combined with solid or molten rock, but there is no satisfactory estimate of the amount of water thus locked up.

As shown in Fig. 12.2 about $1,350 \times 10^{15} \text{ m}^3$ of water (about 97% of all the water in the hydrosphere) is contained in the oceans; while $33.6 \times 10^{15} \text{ m}^3$ (the remaining 2.4%) is found on and in the continents, mostly in the glaciers of the Arctic and the Antarctic. The atmosphere contains $0.013 \times 10^{15} \text{ m}^3$ or only one hundred-thousandth of the total water present on the earth. The transfer rates between the various reservoirs are also shown in Fig. 12.2. They are associated mainly with precipitation, evaporation, and runoff which were discussed extensively in Sec. 7.6.

The water on the continents is distributed in several reservoirs, namely, in glaciers ($25 \times 10^{15} \text{ m}^3$), ground water ($8.4 \times 10^{15} \text{ m}^3$), lakes and rivers ($0.2 \times 10^{15} \text{ m}^3$), and in the living matter of the biosphere ($0.0006 \times 10^{15} \text{ m}^3$). The amount of water locked in the polar ice is impressively large, totaling some 1.8% of all the water in the hydrosphere. Of the total amount of underground water, vadose water (water present in soils) accounts for only $0.066 \times 10^{15} \text{ m}^3$. The remainder is almost evenly divided between reservoirs deeper than 800 m and reservoirs shallower than that level (for an extensive review of the world water resources, see L'vovich and Ovtchinnikov, 1964, and L'vovich, 1979).

The distribution of terrestrial water has slowly changed with time. For instance, continental ice caps have periodically grown and melted during the past two million years. Such fluctuations must, of course, have been accompanied by profound changes in the hydrological cycle.

The residence time of water in the various reservoirs can be deduced from the ratio of the amount of water in the particular reservoir and the accumulation or depletion rate as presented in Fig. 12.2. It is found to vary from about ten days for atmospheric water vapor to thousands of years for the polar ice and the oceans.

12.2 EQUATIONS OF HYDROLOGY

12.2.1 Classic equation of hydrology

The classic equation of hydrology is obtained as a water balance requirement for the terrestrial branch of the hydrological cycle. Applying the principle of continuity to a specific region, the balance equation for the terrestrial branch may be written as

$$S = P - E - R_0 - R_u, \quad (12.1)$$

where

S = rate of storage of water,

P = precipitation rate (in liquid and solid phase),

E = evaporation rate (which includes evapotranspiration over land and sublimation over snow and ice),

R_0 = surface runoff, and

R_u = subterranean runoff.

For a large land region, the net subterranean runoff is usually small so that the classic equation can be simplified to the form

$$\{\bar{S}\} = \{\bar{P} - \bar{E}\} - \{\bar{R}_0\}, \quad (12.2)$$

where $(\bar{\quad})$ denotes a time average and $\{\quad\}$ a space average over the region of area A , $\{\bar{S}\}$ is the rate of change of total surface and subterranean water storage, $\{\bar{P} - \bar{E}\}$ is the average rate of precipitation minus evaporation per unit area, and $\{\bar{R}_0\}$ is the average rate of runoff. For long periods of time and large areas $\{\bar{S}\}$ tends to be small compared to the other terms, and Eq. (12.2) can be reduced to

$$\{\bar{E}\} = \{\bar{P}\} - \{\bar{R}_0\}. \quad (12.3)$$

Traditionally, the quantity of major interest for hydrology has been runoff which can be measured fairly accurately through gauging the extensive network of streams. Precipitation is the primary cause for runoff. As we have seen in Tables 7.1 and 7.2, these two quantities, R_0 and P , are measured and recorded over many continental areas of the globe.

Measurements of evaporation, evapotranspiration, and the change in water storage are very difficult to make, although some semi-empirical estimates of these quantities are available for local areas. Since there is an increasing need for large-scale estimates of evapotranspiration and soil moisture storage for the planning of more efficient irrigation systems, for various water resource projects and, in general, for the optimum use of the available water, hydrologists are now beginning to study the atmospheric branch of the water cycle.

12.2.2 Balance equation for water vapor

The formulation of the atmospheric branch of the hydrological cycle is based on the balance requirements of water vapor in the atmosphere. We will follow the general discussions of Peixoto (1973) and Peixoto and Oort (1983).

The amount of water vapor contained in a unit area column of air which extends from the earth's surface to the top of the atmosphere is given by the expression

$$W(\lambda, \phi, t) = \int_0^{p_0} q \frac{dp}{g}, \quad (12.4)$$

where q is the specific humidity. The term W can be called the amount of precipitable water in the atmosphere. It represents the amount of liquid water that would result if all the water vapor in the unit column of the atmosphere were condensed. It is usually expressed in units of g cm^{-2} or cm . By integrating the horizontal transport of water vapor with respect to pressure the "aerial runoff" \mathbf{Q} is obtained:

$$\mathbf{Q}(\lambda, \phi, t) = \int_0^{p_0} q \mathbf{v} \frac{dp}{g} = Q_\lambda \mathbf{i} + Q_\phi \mathbf{j}. \quad (12.5)$$

The zonal and meridional components of \mathbf{Q} are given by

$$Q_\lambda = \int_0^{p_0} q u \frac{dp}{g} = \langle qu \rangle p_0/g,$$

$$Q_\phi = \int_0^{p_0} q v \frac{dp}{g} = \langle qv \rangle p_0/g.$$

The term Q_ϕ represents the flux of water vapor across a unit strip of a latitudinal wall ($\phi = \text{constant}$) and Q_λ the flux across a unit strip of a meridional wall ($\lambda = \text{const}$). The previous equations may be averaged in time leading to the corresponding mean values \bar{W} , $\bar{\mathbf{Q}}$, \bar{Q}_λ , and \bar{Q}_ϕ .

When the basic balance equation for water vapor (3.79) and the mass continuity equation (3.4) in the (x, y, p, t) system are combined, the budget of water vapor in the atmosphere can be expressed by the following balance equation:

$$\frac{\partial q}{\partial t} + \text{div } q\mathbf{v} + \frac{\partial(q\omega)}{\partial p} = s(q) + D, \quad (12.6)$$

where the source-sink term $s(q)$ equals the rate of generation or destruction of water vapor within a unit mass of air associated with phase changes, and $D = -\alpha \text{div } \mathbf{J}_q^D$ the molecular and turbulent eddy diffusion through the boundaries. The main sources and sinks of water vapor in the atmosphere are primarily evaporation and condensation and, to a lesser extent (except near the earth's surface), diffusion from the surroundings. Thus, $s(q) = e - c$, where e is the rate of evaporation (plus sublimation) and c the rate of condensation per unit mass (in units of g of water per kg moist air per second).

Similarly as for water vapor, we can write a balance equation for the condensed phase (liquid plus solid) q_c , noting that the rate of formation in clouds is given by $s(q_c) = -s(q)$, so that

$$\frac{\partial q_c}{\partial t} + \text{div } q_c\mathbf{v} + \frac{\partial q_c\omega_c}{\partial p} = -(e - c). \quad (12.7)$$

In this equation, ω_c is the vertical velocity of the water droplets or snow and solid ice particles and $q_c\omega_c$ the net vertical transport of the condensed water.

A balance equation for the total water content is obtained by adding Eqs. (12.6) and (12.7):

$$\begin{aligned} \frac{\partial q}{\partial t} + \text{div } q\mathbf{v} + \frac{\partial(q\omega)}{\partial p} + \frac{\partial q_c}{\partial t} \\ + \text{div } q_c\mathbf{v} + \frac{\partial q_c\omega_c}{\partial p} = D. \end{aligned} \quad (12.8)$$

Vertical integration of this equation with respect to pressure between the earth's surface and the top of the atmosphere gives the balance equation for the total water substance in the atmosphere:

$$\frac{\partial W}{\partial t} + \text{div } \mathbf{Q} + \frac{\partial W_c}{\partial t} + \text{div } \mathbf{Q}_c + P = E, \quad (12.9)$$

where W_c is the amount of condensed water in a unit area column of air:

$$W_c(\lambda, \phi, t) = \int_0^{p_n} q_c dp/g \quad (12.10)$$

and \mathbf{Q}_c the horizontal transport vector of condensed water:

$$\mathbf{Q}_c(\lambda, \phi, t) = \int_0^{p_n} q_c\mathbf{v} dp/g = Q_{c\lambda}\mathbf{i} + Q_{c\phi}\mathbf{j}. \quad (12.11)$$

Usually $\partial W_c/\partial t \ll \partial W/\partial t$ and $\mathbf{Q}_c \ll \mathbf{Q}$ so that both the time rate of change of the liquid and solid water in clouds and their horizontal transports can be neglected in Eq. (12.9). Thus, we can simplify the general balance equation after averaging in time to

$$\frac{\partial \bar{W}}{\partial t} + \text{div } \bar{\mathbf{Q}} = \bar{E} - \bar{P}. \quad (12.12)$$

A possible exception is the case of the formation of dense cumulonimbus clouds in the tropics or over warm ocean currents, such as the Gulf Stream and Kuroshio currents during winter (Peixoto, 1973).

Equation (12.12) shows that the excess of evaporation over precipitation at the earth's surface is balanced by the local rate of change of water vapor storage $\partial W/\partial t$ and by the inflow or outflow of water vapor, $\text{div } \mathbf{Q}$. Averaging of Eq. (12.12) in space over a region bounded by a conceptual vertical wall (e.g., a river-drainage basin or an interior sea) leads to another form of Eq. (12.12):

$$\left\{ \frac{\partial \bar{W}}{\partial t} \right\} + \{ \text{div } \bar{\mathbf{Q}} \} = \{ \bar{E} - \bar{P} \}. \quad (12.13)$$

Using the Gauss theorem, Eq. (12.13) may be rewritten in a form, which is often more useful for regional studies:

$$\left\{ \frac{\partial \bar{W}}{\partial t} \right\} + (1/A) \oint (\bar{\mathbf{Q}} \cdot \mathbf{n}) d\gamma = \{ \bar{E} - \bar{P} \}, \quad (12.14)$$

where A denotes the area of the region and \mathbf{n} the unit vector directed outward, normal to the boundary of the region.

Equations (12.13) and (12.14) describe the atmospheric branch of the hydrological cycle. Except in the case of severe storms and for short intervals of time, the rate of change of precipitable water $\partial W/\partial t$ is very small compared with the other terms. Thus, for sufficiently long periods of time, divergence of water vapor is found over those regions of the globe where evaporation exceeds precipitation, whereas convergence is found where precipitation is greater than evaporation.

The term $\{ \bar{E} - \bar{P} \}$ is common to Eqs. (12.2) and (12.13) and establishes the connection between the terrestrial and atmospheric branches of the hydrological cycle. Elimination of $\{ \bar{E} - \bar{P} \}$ between these two equations yields

$$\{ \bar{R}_0 \} + \{ \bar{S} \} = - \{ \text{div } \bar{\mathbf{Q}} \} - \left\{ \frac{\partial \bar{W}}{\partial t} \right\}, \quad (12.15)$$

which shows how the two branches of the hydrological cycle are linked together.

If, besides the aerological terms, $\{ \bar{R}_0 \}$ and $\{ \bar{P} \}$ are known over a certain catchment basin from stream flow and precipitation data, one can estimate the rate of change in ground water and the rate of evaporation. Thus, using finite differences as is usually done in hydrology, Eq. (12.15) may be written

$$\{ \bar{S} \} = - \{ \overline{\Delta W / \Delta t} \} - (1/A) \oint (\bar{\mathbf{Q}} \cdot \mathbf{n}) d\gamma - \{ \bar{R}_0 \}. \quad (12.16)$$

Similarly the mean evaporation can be obtained from Eq. (12.14):

$$\{ E \} = \{ \overline{\Delta W / \Delta t} \} + (1/A) \oint (\bar{\mathbf{Q}} \cdot \mathbf{n}) d\gamma + \{ \bar{P} \}. \quad (12.17)$$

Over long periods of time, such as a year, changes in storage in the land and in the atmosphere become small so that, e.g., for a continent the surface and subsurface runoff have to be exactly balanced by the aerial "runoff" into the continent from the surrounding ocean areas.

When the entire global atmosphere is considered over a long period of time, all transport and storage terms vanish, and we can conclude from Eq. (12.12) that the global-mean evaporation has to be equal to the global-mean precipitation.

12.2.3 Modes of water vapor transport

The water balance equation (12.12) for a zone bounded by the latitudes ϕ and $\phi + \Delta\phi$ can be written as

$$\frac{\partial[\overline{W}]}{\partial t} + \Delta[\overline{Q}_\phi] \cos \phi / R \cos \phi \Delta\phi = [\overline{E} - \overline{P}], \quad (12.18)$$

where $Q_\phi = \int_0^{p_0} qv \, dp/g$. To get a better understanding of the various mechanisms responsible for the global transports of atmospheric water vapor we will expand the zonally averaged transports in the space-time domain (Starr and Peixoto, 1971), similarly as was done before in the case of angular momentum.

For example, for the mean northward transport of water vapor across a specific latitude circle at a certain pressure level we may use expansion (4.9):

$$[\overline{qv}] = [\overline{q}][\overline{v}] + [\overline{q^*v^*}] + [\overline{q'v'}]. \quad (12.19)$$

Here, the term $[\overline{q}][\overline{v}]$ represents the transport of water vapor by the mean meridional circulation which dominates in the tropics. The term $[\overline{q^*v^*}]$ is associated with the mean stationary eddies of the general circulation, such as the semipermanent subtropical anticyclones and the semipermanent cyclones prevailing in high latitudes. Finally, the term $[\overline{q'v'}]$ represents the northward transport of moisture due to the transient perturbations which develop along the polar front and in the intertropical convergence zone.

Integration of Eq. (12.19) in the vertical then leads to the expansion of the total meridional transport in terms of the various modes of transfer:

$$\begin{aligned} [\overline{Q}_\phi] &= (1/g) \int [\overline{q}][\overline{v}] \, dp \\ &\quad + (1/g) \int [\overline{q^*v^*}] \, dp + (1/g) \int [\overline{q'v'}] \, dp. \end{aligned} \quad (12.20)$$

Similarly we can consider the vertical transport of water vapor $q\omega$ and expand its zonal and time mean into the various components

$$[\overline{q\omega}] = [\overline{q}][\overline{\omega}] + [\overline{q^*\omega^*}] + [\overline{q'\omega'}]. \quad (12.21)$$

The vertical transport of moisture constitutes a link between the earth's surface and the free atmosphere, providing water vapor and latent heat to the upper levels of the atmosphere. The transient eddy term $[\overline{q'\omega'}]$ describes the vertical transfer of water vapor due to turbulent diffusion, cumulus convection, and other mesoscale convective phenomena. A similar expression as Eq. (12.21) can be derived for the condensed phase. In that case the term $[\overline{q_c\omega_c}]$ represents the vertical transport of water droplets or solid ice particles, which, in general, is downward when $[\overline{q\omega}]$ is upward. It represents the rate of precipitation at a given pressure level.

12.3 OBSERVED ATMOSPHERIC BRANCH OF THE HYDROLOGICAL CYCLE

12.3.1 Water vapor in the atmosphere

12.3.1.1 Precipitable water

The annual-mean distribution of the specific humidity near the surface expressed in g's of water vapor per kg of moist air is shown in Fig. 12.3(a). As expected, the highest humidities of 18 to 19 g kg⁻¹ are found in the equatorial regions. There is a continuous decrease of humidity with latitude down to very low values on the order of 1 g kg⁻¹ or less over the polar regions. The global pattern of humidity resembles the temperature patterns in Fig. 7.4(a) since the capacity of the atmosphere to retain water vapor depends strongly on temperature. Of course, there are exceptions in the major desert regions where the surface air is very dry compared to the zonally averaged humidity in spite of its relatively high temperature.

The January minus July difference map of the surface specific humidity in Fig. 12.3(b) shows that the largest annual variations occur in relatively low latitudes over the continents. The variations associated with the Asian monsoon are also very pronounced. Comparing this difference map of specific humidity with the corresponding map of surface temperature in Fig. 7.4(c) we recognize that similar features appear on both maps. However, in the case of humidity the centers are displaced equatorward by about 15° latitude over North Africa, 30° latitude over Asia and North America, and 10° latitude over the Southern Hemisphere continents.

The spatial distribution of the annual-mean precipitable water content \bar{W} is represented in Fig. 12.3(c). With only a few exceptions, the analysis shows a continuous decrease of precipitable water from the equatorial regions, where it attains the highest values, to the north and south poles.

The departures from zonal symmetry are associated with the physiography of the earth's surface, and are apparent in both hemispheres. As a general rule, the precipitable water is higher over the oceans than over the continents. The deflection of the isolines near the western and eastern coasts of the continents is reinforced by the topography and the presence of warm and cold ocean currents. The distribution over the Southern Hemisphere is practically zonal, since the ocean coverage exceeds by far that of the continents. As expected, the lowest values of \bar{W} (< 5 kg m⁻²) occur over subpolar and polar regions.

The precipitable water over the desert areas is considerably smaller than the corresponding zonal average, mainly due to strong subsidence. This effect is pronounced in the eastern portions of the large semipermanent anticyclones of the subtropics. In addition, the effects of high terrain on the precipitable water distribution are illustrated by relatively dry areas (often $\bar{W} < 10$ kg m⁻²) over the major mountain ranges, such as the Rockies, Himalayas, highlands of Ethiopia, and the Andes. The effects of topography and the land-sea contrast in the Southern Hemisphere are shown by the dipping of the 20 kg m⁻² isoline towards lower latitudes.

It is also useful to consider water vapor in terms of the relative humidity of the air U , given by the ratio of the actual vapor pressure and the saturation vapor pressure [see Eq. (3.62)]. Figure 12.3(d) shows the horizontal distribution of relative humidity in the lower troposphere for annual-mean conditions. It clearly shows the humid

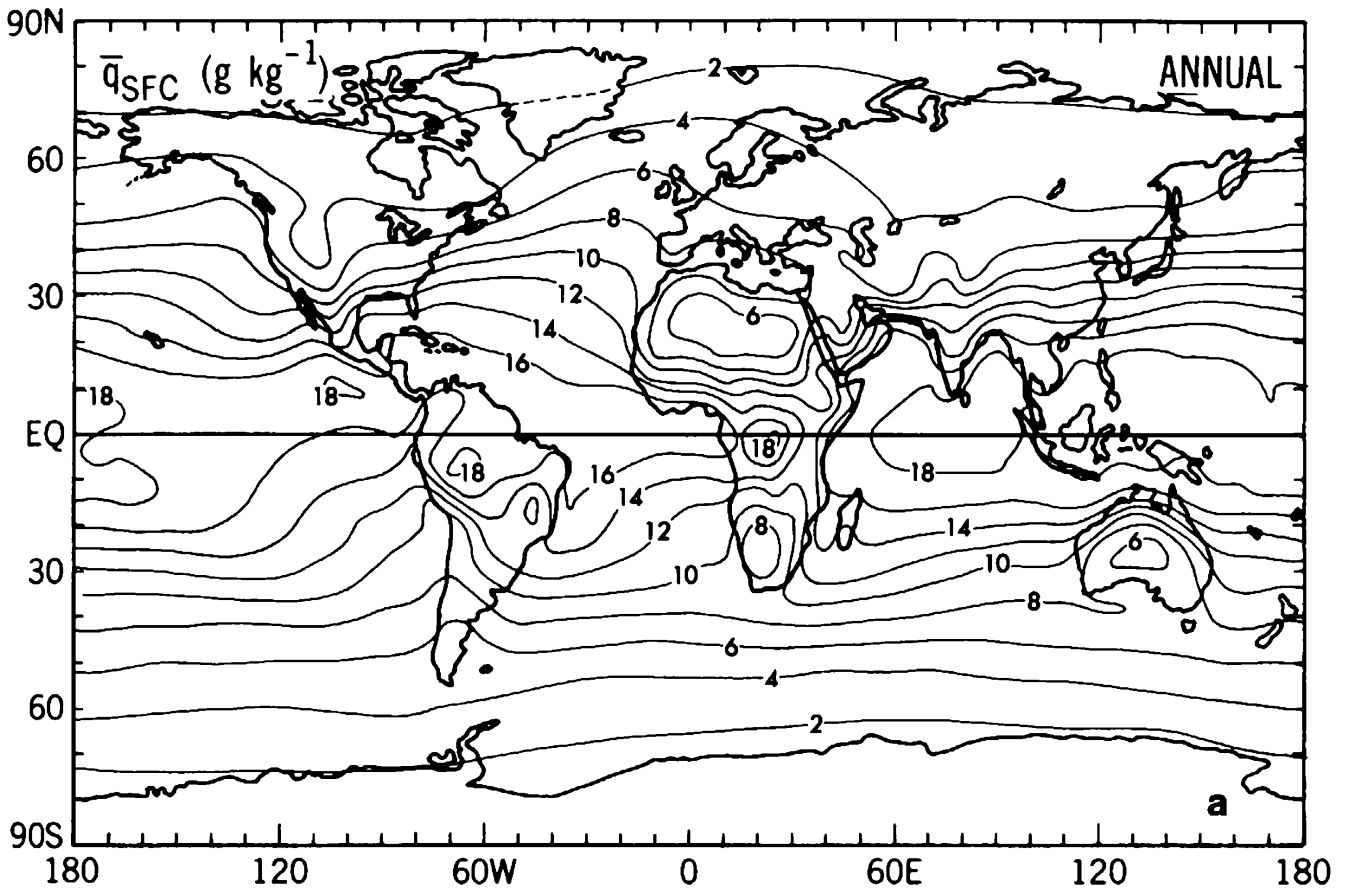


FIGURE 12.3a

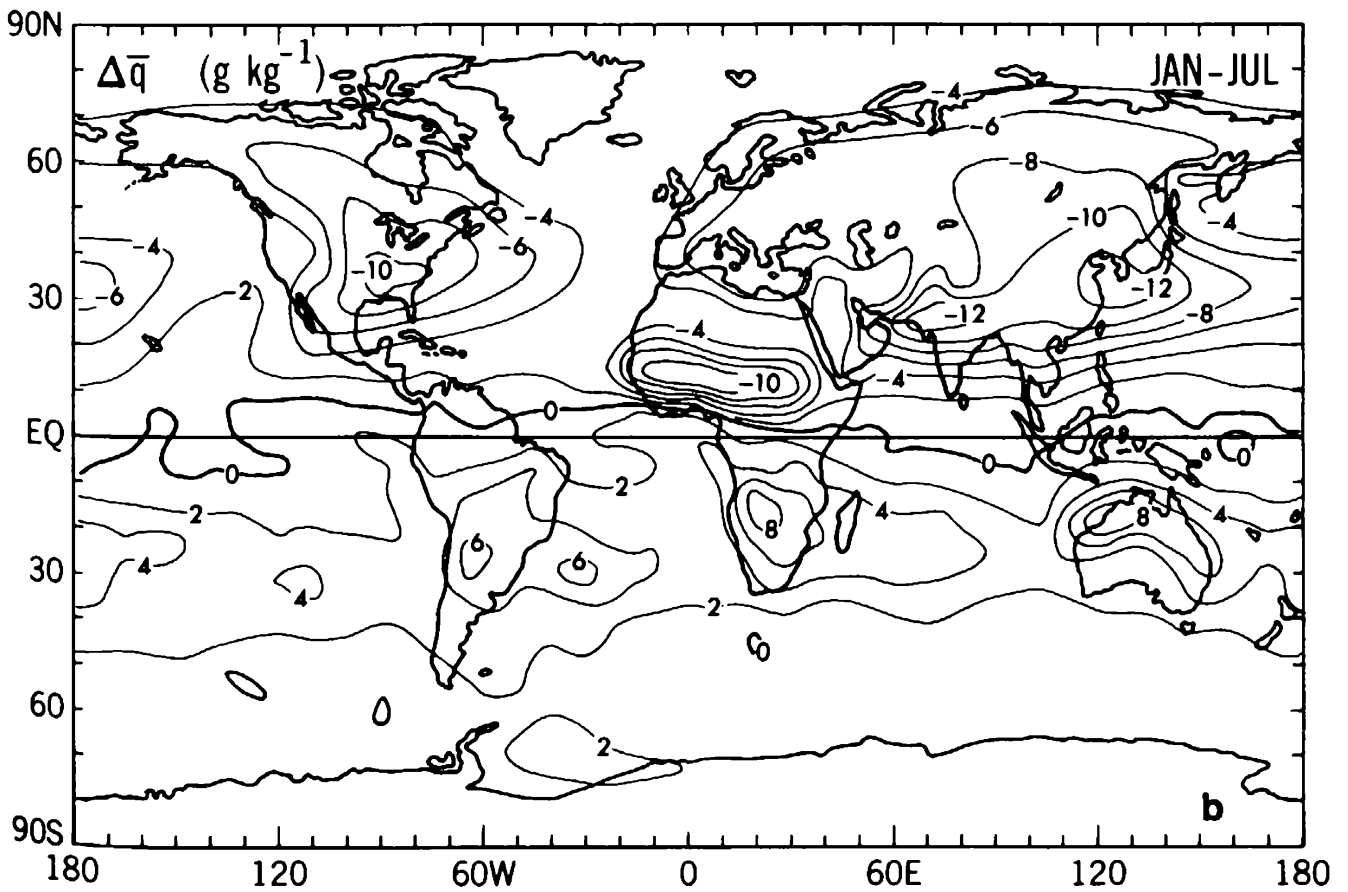


FIGURE 12.3b

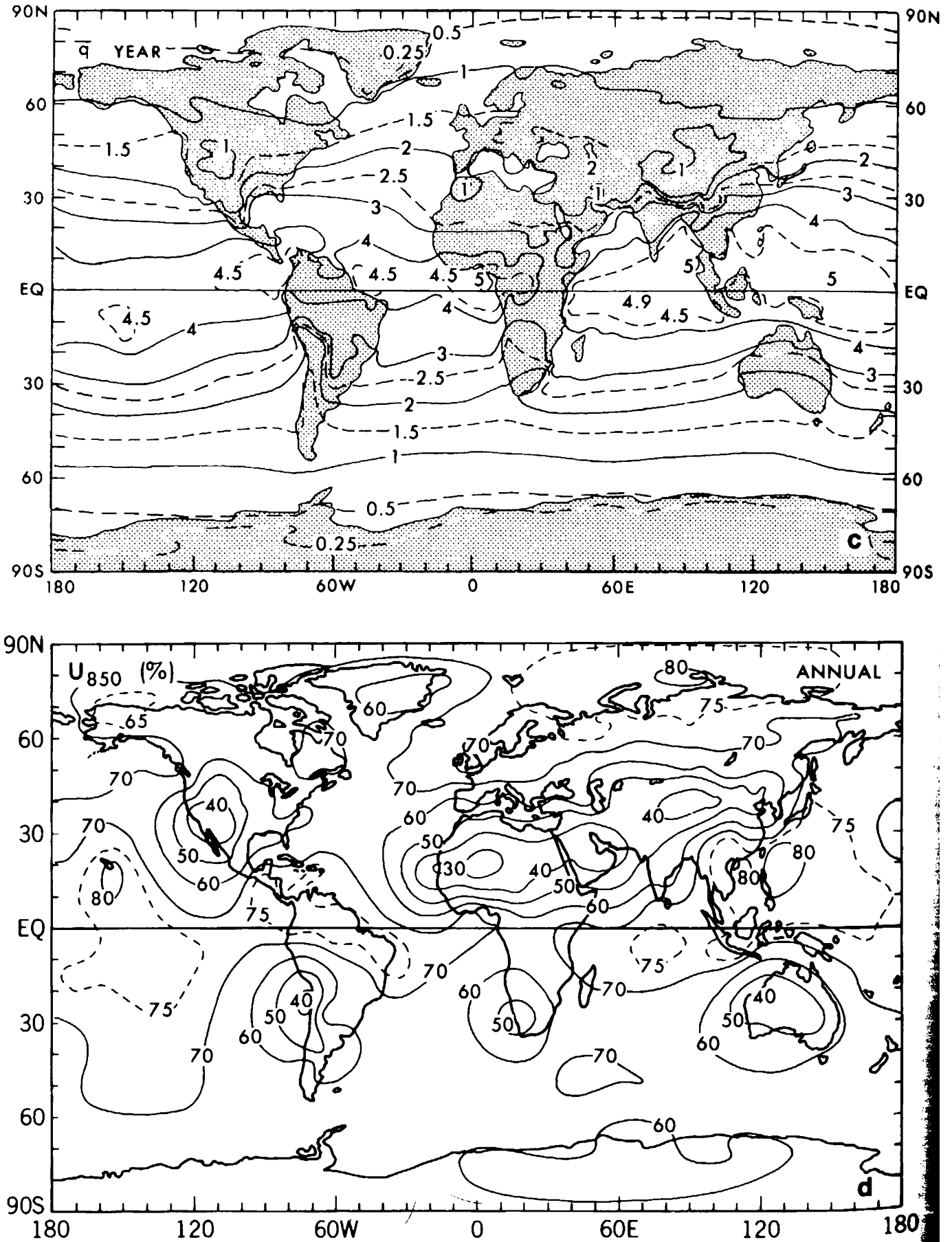


FIGURE 12.3. Global distributions of the surface specific humidity for annual-mean (a) and January-minus-July conditions (b), of the vertical-mean specific humidity (c) in g kg^{-1} , and of the relative humidity (d) at 850 mb in %. [When multiplied by p_0/g (≈ 1 over the oceans and low-level land areas) the third field gives the precipitable water in the atmosphere in units of 10 kg m^{-2} .]

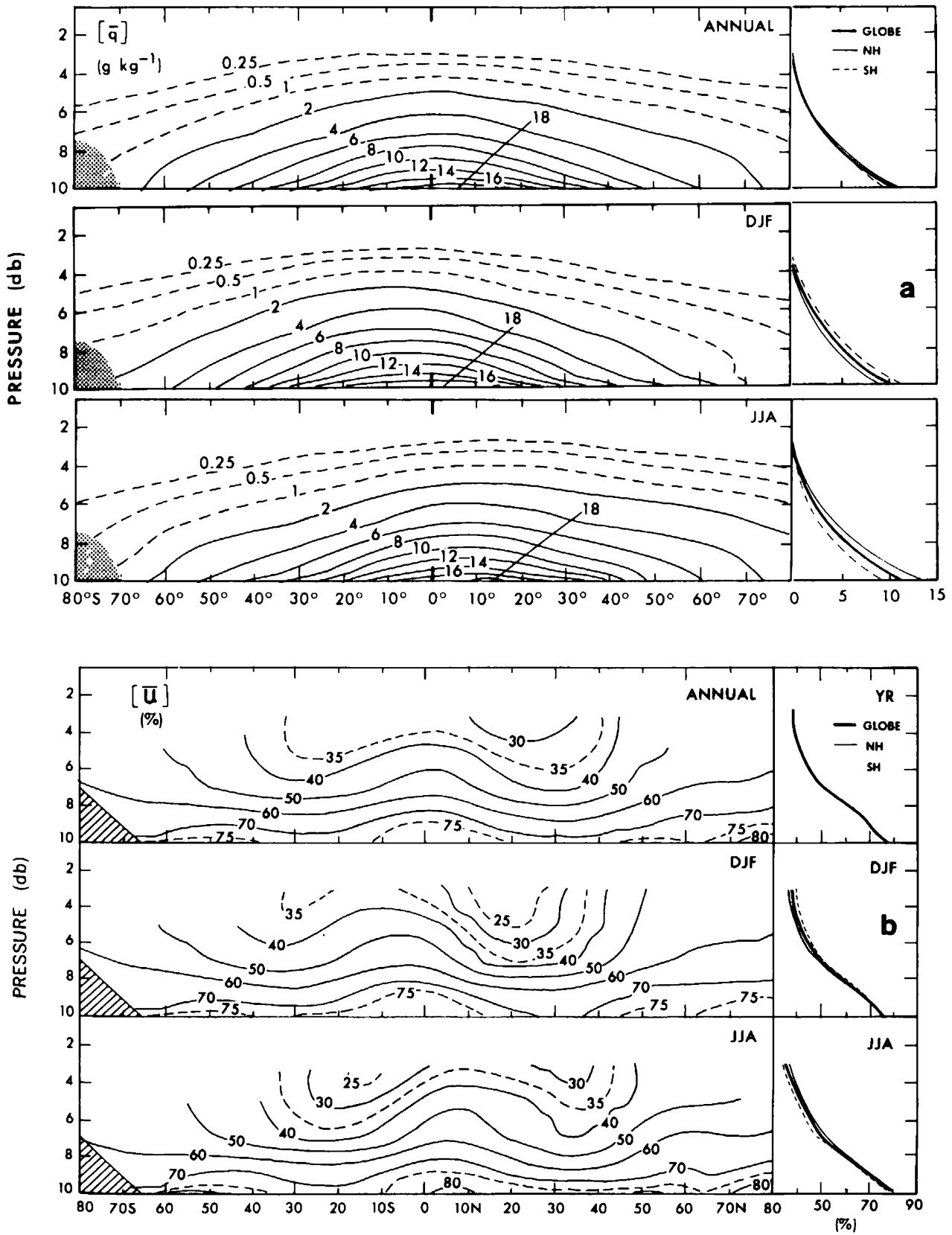


FIGURE 12.4. (a) Zonal-mean cross sections of the specific humidity in g kg^{-1} for annual, DJF, and JJA mean conditions. Vertical profiles of the hemispheric and global mean values are shown on the right. (b) Zonal-mean cross sections of the relative humidity in % for annual, DJF, and JJA mean conditions.

equatorial regions with values on the order of 75% and the dry subtropical regions with minimum values of 30%–40% over the continental deserts. As expected, the relative humidity is higher, in general, over the oceans than over land.

The vertical structure of water vapor is shown in Figs. 12.4(a) and 12.4(b) in the form of zonal-mean cross sections of the mean specific humidity $[\bar{q}]$, and the mean relative humidity $[\bar{U}]$, respectively. The specific humidity decreases rapidly with height, almost following an exponential law as shown in the vertical profiles on the right-hand side of Fig. 12.4(a). It also decreases with latitude. More than 50% of the water vapor is concentrated below the 850-mb surface, while more than 90% is confined to the layer below 500 mb. The seasonal variations are more intense in the Northern than in the Southern Hemisphere, as expected from the corresponding temperature variations.

The cross sections of relative humidity in Fig. 12.4(b) also show a decrease with height but weaker than in the case of specific humidity. The relative humidity ranges from values on the order of 70% to 80% near the surface to 30%–50% near the 400-mb level. The latitudinal gradients tend to increase with height, reflecting the influence of the rising and sinking branches of the mean meridional circulation (see Figs. 7.18 and 7.19). Thus, in the annual mean, strong sinking motions near 20°–30° latitude lead to a minimum in relative humidity at those latitudes in each hemisphere, whereas the rising motions in the ITCZ give rise to the maximum just north of the equator. The seasonal differences in intensity and location of the Hadley cells are clearly reflected in the latitudinal shifts from about 25° latitude in winter to 35° latitude in summer. The seasonal range has a maximum of $\Delta U \simeq 15\%$ – 20% near 15° latitude in each hemisphere at the 500-mb level.

The variability in time and space of the vertical moisture distribution is portrayed in Figs. 12.5(a)–12.5(d) for annual-mean and seasonal conditions. Figures 12.5(a) and 12.5(c) represent the intra-annual (seasonal and synoptic) temporal variability

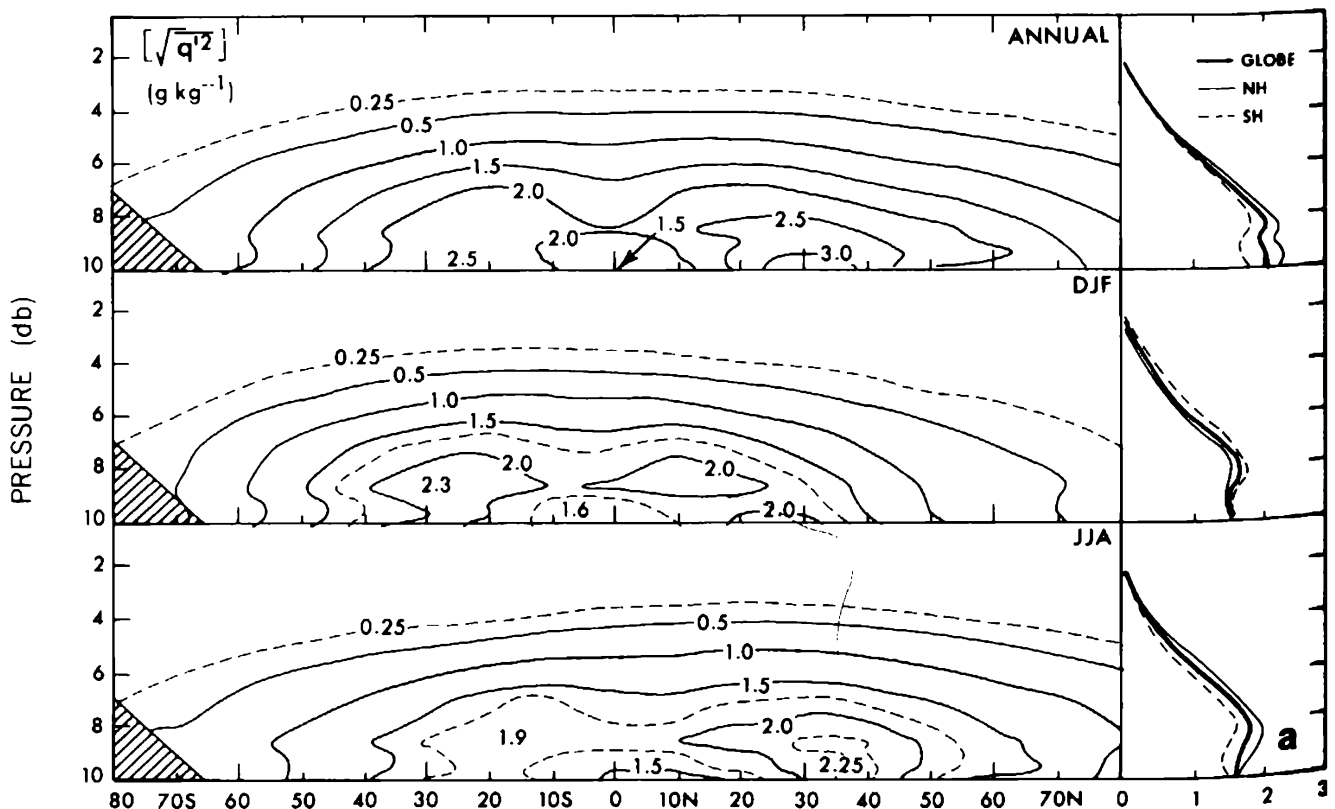


FIGURE 12.5a